Adam BIERNAT

Warsaw University of Technology, Institute of Control and Industrial Electronic

doi:10.15199/48.2017.02.02

Coil-turn short-circuit of PMSM influence on the transformed phase voltage frequency pattern

***Abstract**. In the paper the possibility of detection of PMSM stator winding turn short-circuit based on changes in transformed phase voltage in generating no-load state of operation is discussed. For this purpose analysis of induced voltage space phasor magnitude time change is used. Diagnostic data is obtained from experimental testing of PMSM designed for electrical car application.*

***Streszczenie.** W artykule przeanalizowano możliwość diagnozowania zwarcia zwojowego maszyny synchronicznej z magnesami trwałymi w oparciu o zmiany zachodzące w transformowanym napięciu fazowym podczas pracy generatorowej w stanie jałowym. Analizie poddana została zmienność czasowa modułu fazora przestrzennego napięcia indukowanego. Pomiary diagnostyczne zostały zrealizowane podczas testów laboratoryjnych silnika synchronicznego zaprojektowanego do bezpośredniego napędu samochodu elektrycznego. (**Wpływ zwarcia zwojowego na podstawie w Silniku Synchronicznym Magnesami trwałymi na obraz widma transformowanego napięcia fazowego**).*

Keywords: permanent magnet synchronous machine, diagnostics, turn short-circuit fault detection, signal analysis.
Słowa kluczowe: silnik synchroniczny z magnesami trwałymi, diagnostyka, wykrywanie zwarcia zwojowego, analiza sygnału.

Introduction

Technical fitness of device and it's user safety could be achieved by possibly frequent monitoring device technical condition. If technical device contains electrical machine/machines it is necessary to encompass them by monitoring process. Periodic diagnostic tests (that enable formulating proper diagnostic verdict and launching if necessary emergency procedure) require satisfying stationarity condition of diagnostic signal while keeping possibly similar extortions. For this reason diagnostic tests are performed in such a periods of variable work cycle that meet above requirements. Suggested period of work cycle in case of electrical machine could be for example locked rotor state [1] or no load state of operation. In the paper possibility of PMSM winding turn short-circuit diagnosis in no load generating state of operation is discussed. Diagnostic signal is instantaneous value of voltage space phasor magnitude.

Detection of coil-turn short-circuit on the base of induced voltage dissymmetry

Turn short-circuit is rated among most frequently occurred electrical machines failure [2]. Owing to rapid development of such failure only possibly early detection allows to avoid machine breakdown. On the other hand early detection is troublesome due to the fact that in early stage of development turn short-circuit has negligible influence on machine operation. Turn short-circuit leads to local air gap flux dissymmetry as a result of appearance of short-circuit current in shorted winding turn forced by voltage induced by resultant flux.

This dissymmetry which could be described by additional forward and backward rotating flux component that should appear also in phase induced voltage. Attention should be turned on fact that positive and negative component of particular phase voltage spectrum frequency caused by turn short-circuit reveals only through the change of its amplitude (small in the beginning of failure development) that may lead to non unambiguous diagnostic verdicts. Induced voltage dissymmetry reveals in deformation of space phasor loci [3] obtaining by transformation of three-phase voltages u_{fa}, u_{fb}, u_{fc} arrangement in to orthogonal two-phase voltage u_{d}, u_{q} arrangement with fixed position of reference axes with respect to stator:

$$\{u_{fa}, u_{fb}, u_{fc}\} \rightarrow \{u_{d}, u_{q}\} \tag{1}$$

Deformation of space voltage phasor loci reveals time and space variations of space phasor magnitude:

$$u_{dq}(\alpha,t) = \sqrt{(u_{d}(t))^2 + (u_{q}(t))^2} \tag{2}$$

Orthogonal two-phase voltage signal:

$$\begin{aligned} u_{d}(t) &= \sum_{l=1}^{L} U_l^{d} \cos(\omega_l t + \varphi_l) \\ u_{q}(t) &= \sum_{l=1}^{L} U_l^{q} \cos(\omega_l t + \varphi_l) \end{aligned} \tag{3}$$

where: l = 1, 2, 3,…L, U_l^{d}, U_l^{q} – amplitudes of frequency components of order l, respectively for orthogonal signal of d and q axes, ω_l, φ_l - pulsation and phase of frequency components of order l,

contains frequency components that exists in three-phase signal. However space voltage phasor magnitude contains new common-differential frequency components:

$$\begin{aligned} |f(\phi,t)| &= \sqrt{\left(\sum_{l=1}^{L} A_l^{d}\cos(\omega_l t+\varphi_l)\right)^2 + \left(\sum_{l=1}^{L} A_l^{q}\cos(\omega_l t+\varphi_l)\right)^2} = \\ &= \left(\sum_{l=1}^{L}\sum_{k=1}^{L}\left(\frac{A_l^{d}A_k^{d}}{2}\left[\cos((\omega_l \mp \omega_k)t + (\varphi_l \mp \varphi_k))\right] + \right.\right. \\ &\left.\left. + \frac{A_l^{q}A_k^{q}}{2}\left[\cos((\omega_l \mp \omega_k)t + (\varphi_l \mp \varphi_k))\right]\right)\right)^{\frac{1}{2}} = \\ &= \left(\sum_{l=1}^{L}\sum_{k=1}^{L}\left(\frac{(A_l^{d}A_k^{d} + A_l^{q}A_k^{q})}{2}\left[\cos((\omega_l - \omega_k)t + (\varphi_l - \varphi_k))\right] + \right.\right. \\ &\left.\left. + \frac{(A_l^{d}A_k^{d} - A_l^{q}A_k^{q})}{2}\left[\cos((\omega_l + \omega_k)t + (\varphi_l + \varphi_k))\right]\right)\right)^{\frac{1}{2}} \end{aligned} \tag{4}$$

Components of equation (4) formed by difference of radian frequency describe positive while sum of radian frequency – negative components of space phasor. Negative and positive components appear as a result of not only amplitude difference of adequate frequency components of three phase signal u_{fa}, u_{fb}, u_{fc}, but also as a result of three phase signal adequate frequency component mutual phase shift change. The last peculiarity explain different sensitiveness of space phasor magnitude time change on three phase voltage dissymmetry than single phase time change.

Disregarding space variation allows to treat signal $u_{dq}(\alpha,t)$ as time depending signal shifted in frequency domain by fundamental harmonic frequency f_1 [4]:

$$u_{dq}(\alpha,t) = u_{dq}(t)e^{-j2\pi f_1 t} \tag{5}$$

Frequency domain signal $u_{dq}(t)$ shift by fundamental harmonic frequency f_1 effectuate in mutual shifting of positive and negative components that exist in phase voltage by frequency $2f_1$.

Simple simulations show proportionality of negative and positive frequency components amplitude both to chosen phase frequency component amplitude change or to chosen phase frequency component phase change. In case of phase voltage odd frequency components divisible by three only negative and positive frequency components appear. In case of phase voltage odd frequency components non divisible by three negative or positive frequency components are over imposed on existing frequency component that may lead to amplitude modifications.

Comparison of spectrum frequency components amplitude of diagnostic signal for healthy motor and motor with turn short-circuit could be replaced by finding differences in picture that presents frequency-frequency map (F-F map) [1]. F-F map is created by presentation of spectrum parts in cascade way [4]:

$$\Delta X(n,m) = X(n + (m-1)M_p) \tag{6}$$

where: n = 1, 2, 3 … N_p, – element of spectrum part, N_p – number of elements in spectrum part, m = 1, 2, 3 ... M_p – spectrum part, M_p –number of spectrum parts,

while height of frequency components are marked by appropriately chosen contour lines. Idea of creation if F-F map is explained on figure 1. 2-D map is created on the base of 3-D map by representing amplitude as contour lines.

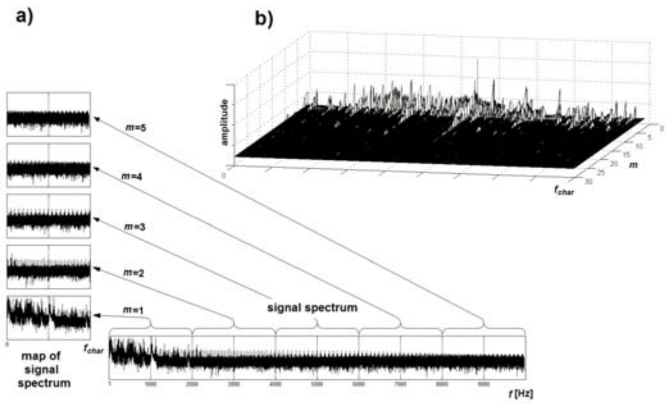

Fig.1. Idea of creation of F-F map: a) assembling of signal spectrum parts, b) resultant 3-D F-F map

Spectrum part range is a chosen characteristic frequency f_{char} (ordinate axe describes subsequent spectrum part, abscissa axe describes frequency range of spectrum part). As a measure of F-F map structure regularization, the mean amplitude value of frequency components of range 0 – f_{char} and its higher harmonics spaced by f_{char}:

$$\Delta X_{sum}(n) = \frac{1}{M_p}\left\{\sum_{m=1}^{M_p} \Gamma[X(n+(m-1)N_p)]\right\} \tag{7}$$

where: Γ– scale change operation of spectrum frequency components amplitude,

determined on the base of spectrum F-F map is proposed [4]. Thus defined amplitude mean value is equivalent to synchronous averaging in frequency domain. Motivation for determining mean amplitude value of frequency components is attempt to create diagnostic measure that characterize high sensitiveness to chosen frequency component and their higher harmonics amplitude change. It is worth to mention that proposed measure comparatively les sensitive to individual component amplitude change.

Analysis of transformed voltage signal of PMSM turn short-circuit

Subject of analysis is low rotational speed, three phase synchronous motor with permanent magnets and outer rotor with p = 17 pair of poles (number of rotor permanent magnets is N_2=34) and N_1=36 stator teeth [5].

Experiment was performed for healthy and motor and turn short-circuit of one concentrated winding coil. Voltage was measured using voltage/voltage sensors with galvanic separation and frequency range 0– 20 kHz for rotational speed 300 rpm.

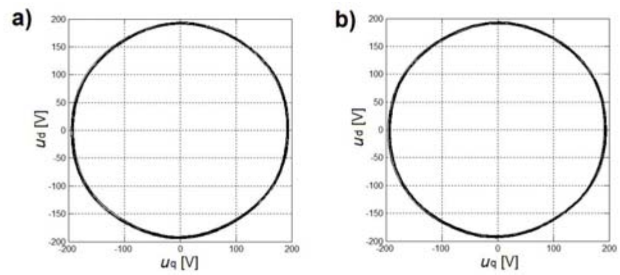

Fig.2. Voltage space phasor loci of PMSM: a) healthy motor, b) motor with turn short-circuit of one concentrated winding coil

Mentioned above weak conditionality dependence between device state feature (arising short-circuit) and diagnostic signal parameters confirms comparison of space phasor loci in case of healthy and faulty motor (fig. 2).

Analysis of voltage space phasor magnitude time variation reveals appearance of side bands distant from fundamental frequency component and it higher harmonics by frequency $N_1 f_1$ determined by tooth-grove stator structure (on fig. 3b only the side bands of fundamental frequency $f1$ are marked). Attention should be turned to existence of third and ninth fundamental frequency harmonic in voltage space phasor magnitude time variation. This indicate that three phase system develops amplitude differences and possibly own mutual non-zero phase shift of odd, divisible by three harmonics due to basic motor dissymmetry.

In the PMSM dominant basic dissymmetry is rotor magnetic circuit dissymmetry developed by tolerance of each individual magnet manufacture. That means that as characteristic frequency common-differential main frequency components (in this case equal to the product of rotational frequency f_w and number of stator teeth N_1) could be adopted. On figure 3 amplitude spectrum of phase voltage and magnitude of voltage space phasor amplitude spectrum with frequency domain shift correction is presented. Frequency shift facilitate comparison with phase voltage amplitude spectrum.

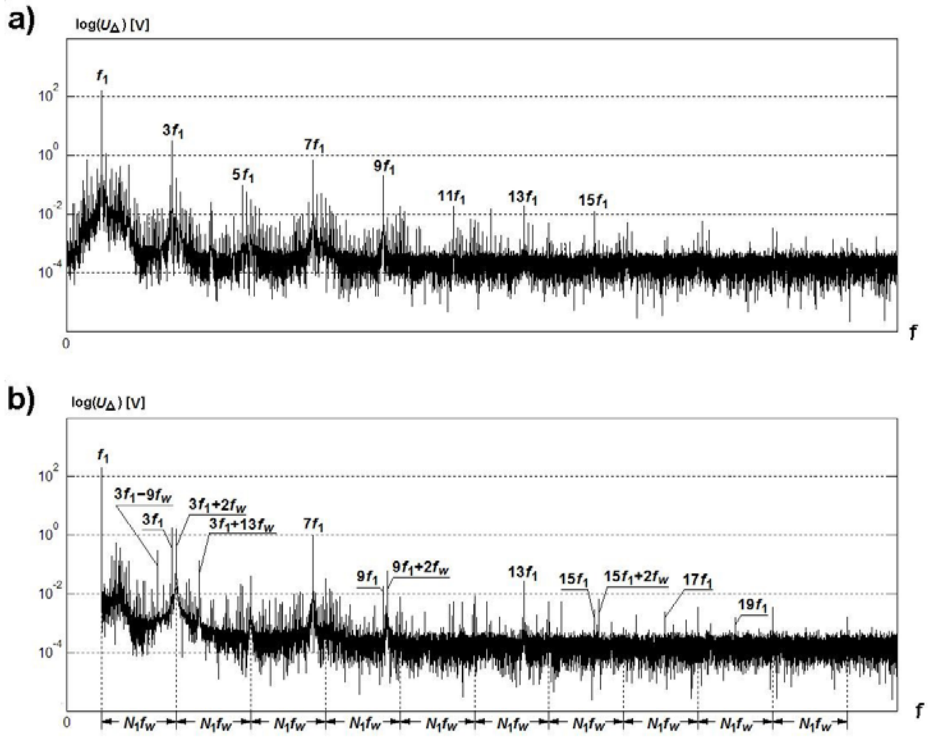

Fig.3. Healthy motor: a) amplitude spectrum of phase voltage, b) spectrum of magnitude of voltage space phasor

On figure 4 F-F maps of voltage space phasor magnitude amplitude spectrum determined according to (1) and (2) for healthy and failed motor, shifted by fundamental frequency f_1 are presented. As characteristic frequency of presented F-F maps double of common-differential frequency components of fundamental frequency $f_1=f_w p$ and rotational frequency f_w that is equal to of product of rotational frequency and number of stator teeth $2(p+1)f_w=(N_2+2)f_w=N_1 f_w$ is adopted. For adopted characteristic frequency F-F maps show highest level of structure regularization. Frequency components distant by characteristic frequency form side bands of different intenseness (in the picture of F-F map side bands are visible as vertical structures distant from each other by rotational frequency f_w and it multiples).

In the spectrum of voltage space phasor magnitude apart of above mentioned frequency components, frequency components (marked by gray area) that create diagonal structure appears. Frequency components that create diagonal structure are distant from each other by multiple of fundamental frequency $f_1=pf_w$. They originate in mutual modulation of fundamental and higher phase voltage harmonics. Frequency of dominating diagonal structure frequencies are as follow: $6f_1=5f_1+f_1=7f_1-f_1$ – common-differential frequency components of fundamental and fifth backward rotating time harmonic or seventh forward rotating time harmonic and $12f_1$ that is common-differential frequency components of first and eleventh or thirteenth time harmonics

Stator turn short-circuit of concentrated coil leads to change in tooth saturation and in consequence increase of stator dissymmetry. Deepening of stator dissymmetry results in amplitude modification of already existing frequency components and appearance of new ones in form of side bands distant by rotational frequency f_w that are grouped in the centre of gray area. What confirms that discussed stator failure deepens amplitude differences between phases odd, divided by three harmonics (in this case ninth).

On the figure 5 the fragment of 3D F-F map containing frequency components that are subject of greatest modifications is presented. Changes in amplitude spectrum originated in turn short-circuit reveal presented on figure 6, determined on the base of F-F map fragment (fig. 5) according to (7) mean values of frequency component amplitude logarithms distant by characteristic frequency. White arrows indicate increase of mean amplitude logarithm values of ninth harmonic of fundamental frequency and its side bands distant by rotational frequency f_w, proving stator dissymmetry increase. It is interesting that some (indicated by black arrows) mean amplitude logarithm values of frequency components (synchronous with frequency $(N_2+2)f_w$)) as explained earlier decrease.

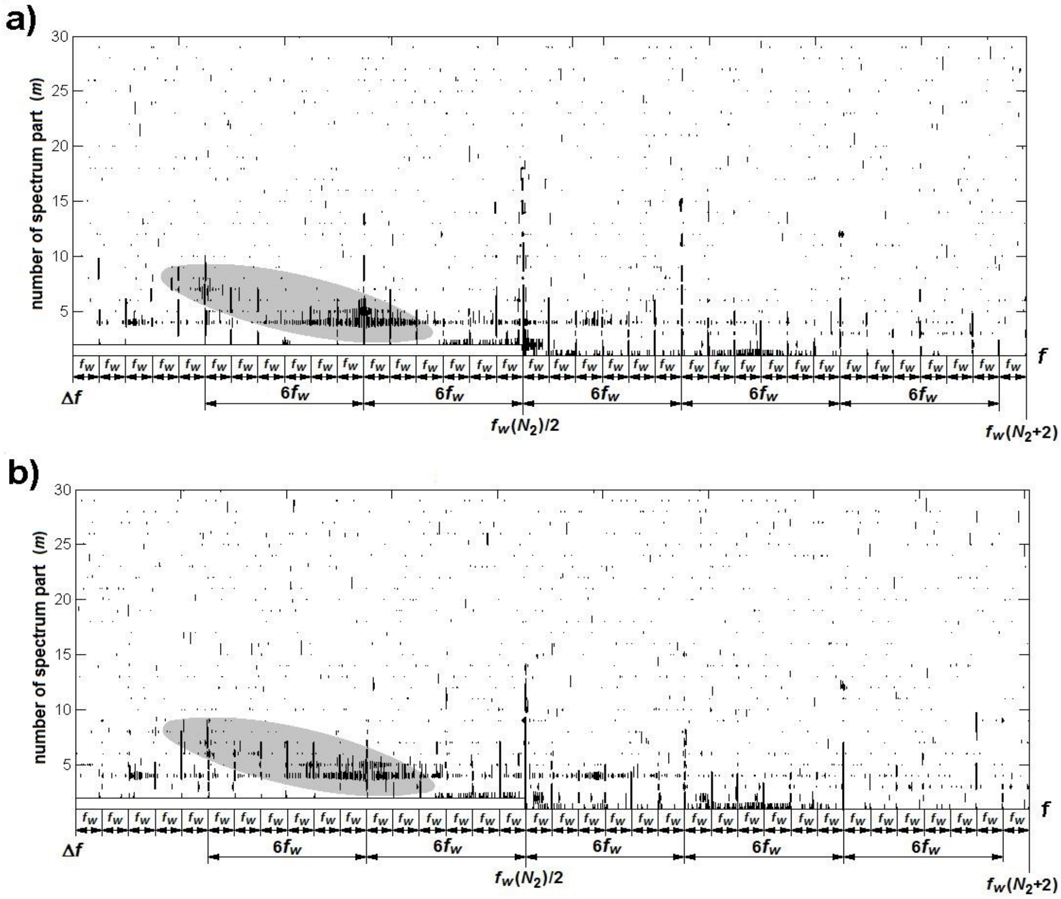

Fig.4. F-F map of magnitude of voltage space phasor spectrum: a) healthy motor, b) motor with turn short-circuit of one concentrated winding coil

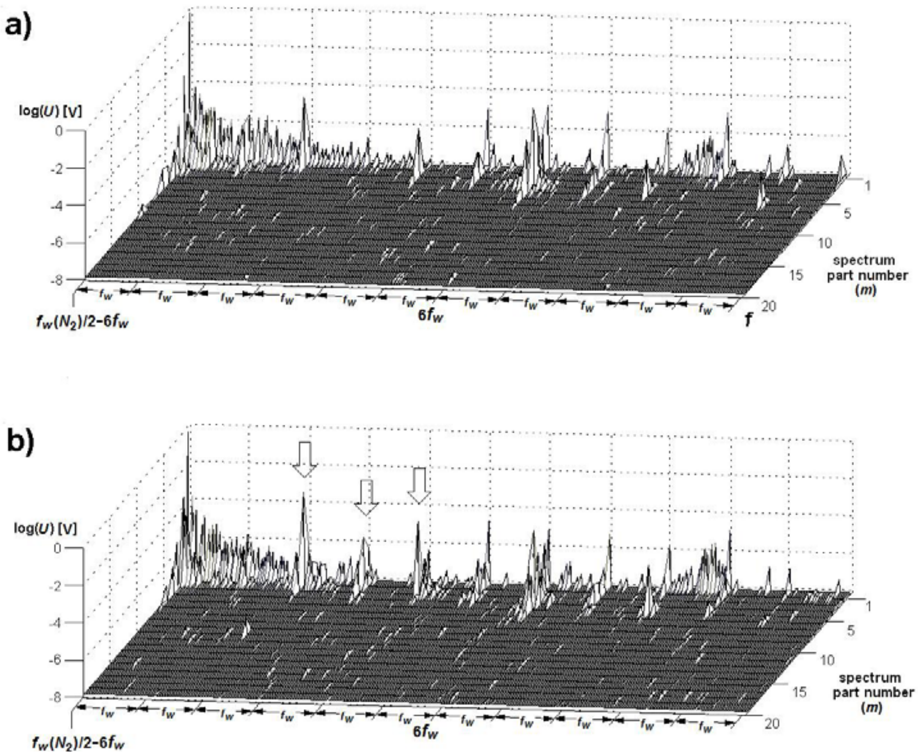

Fig.5. Fragment of 3D F-F map with left sided bands distant by rotational frequency f_w: a) healthy motor, b) motor with turn short-circuit of one concentrated winding coil (arrows indicate side bands which amplitude changes substantially)

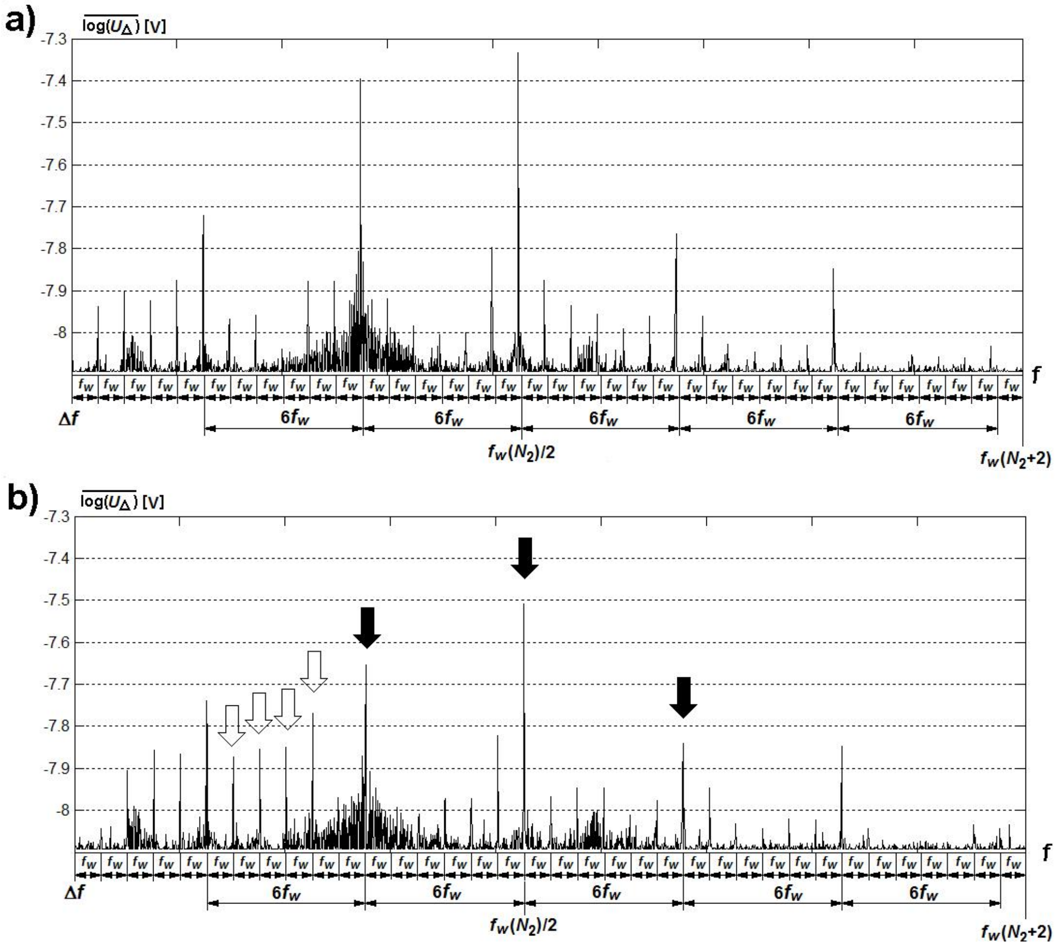

Fig.6. Mean values of frequency component amplitude logarithms distant by characteristic frequency: a) healthy motor, b) Motor with turn short-circuit of one concentrated winding coil

Summary

Presented in the paper method of diagnostics signal analysis enable detection of turn short circuit utilizing measurement of induced voltage in no-load state of operation. Despite of weak conditionality dependence between turn short-circuit and diagnostic signal parameters proposed F-F map of voltage space phasor magnitude spectrum allows to find and interpret signal differences of healthy and faulty motor by narrowing search to particular map area. Diagnostic measure based on mean value of amplitude of frequency components distant by characteristic frequency shows adequate sensitiveness to analyzed machine fault.

***Author**: dr inż. Adam Biernat, Warsaw University of Technology, Institute of Control and Industrial Electronic, Division of Electrical Machines, ul. Koszykowa 75, 00-662 Warszawa, E-mail: adam.biernat@ee.pw.edu.pl.*

REFERENCES

[1] Toliyat H. A., Handi S., Choi S., Meshgin-Kelk H.: Electric Machines – modeling, condition monitoring, and fault diagnosis. *CRC Press*, pp 20-21, pp 226-231 ISBN 978-1-4200-0628-5

[2] Kliman G. B., Premerlani W. J., Koegl R. A., Hoeweler D.: A New approach to on-line turn fault detection in Ac motors. *IEEE Transactions on Energy Conversion*, Vol. 19 Issue 3 (2004) pp 576-582

[3] Dencer A., Jarek T.: Electric Analiza drgań prądnicy z magnesami trwałymi na podstawie generowanego napięcia. *Logistyka* 6/2014, pp 3041-3047.

4] Biernat A.: Analiza sygnałów diagnostycznych maszyn elektrycznych. *Oficyna Wydawnicza Politechniki Warszawskiej*, Warszawa 2015, ISBN 978-83-7814-458-8 pp 49-57

[5] Szczypior J., Jakubowski R., Biernat A.: Ekomobilność – Innowacyjne i ekologiczne środki transportu, Konstrukacja maszyny elektrycznej do bezpośredniego napędu samochodu, Badania maszyny elektrycznej. *Wydawnictwa Komunikacji i Łączności*, Warszawa 2015, ISBN 978-83-1953-9, pp 329-355